Tutor/s

Dra. E. Carolina Sañudo Zotes

Departament de Química Inorgànica i Orgànica

Grau de Química

Treball Final de Grau

Luminescent 2D materials for smart inks

Materials 2D luminescents per tintes intel·ligents

Laura Navarro Spreafico

January 2021

UNIVERSITAT DE BARCELONA

B:KC Barcelona Knowledge Campus
Campus d'Excel·lència Internacional

Mai consideris l'estudi com una obligació,
sinó com una oportunitat per a penetrar
en el bell i meravellós món del saber.
Albert Einstein

Gràcies a la meva família, per haver-me donat la oportunitat d'arribar fins aquí i haver-me recolzat i acompanyat en el procés. Al Guille, per haver-me escoltat i ajudat sempre que he tingut un mal dia. A totes les persones que he conegut al llarg de la carrera, i als amics que he anat fent pel camí, que de ben segur m'emporto per sempre.

Moltes gràcies a la Carolina, per haver-me guiat en tot moment, disposada sempre a ajudar-me i a fer que realment aprengués d'aquest treball. També gràcies a tot el grup de GMMF que han fet que em sentís en tot moment com a casa. Sobretot gràcies a la Rosa, al Guillem, a la Diamantoula i al Jonay, per fer que cada tarda tingués més ganes d'anar al laboratori fent-me sentir com una més.

REPORT

CONTENTS

1. SUMMARY

The increment of documents or currency counterfeiting is being a problem for society, making it necessary to find a solution. One possible method is the development of smart inks, which are luminescent under certain light wavelength.

To do it, metal-organic frameworks (MOFs) with structure $[Ln(CH_3COO)(PhCOO)_2]$ of Ln = Tb, Eu and Sm are used. Homometallic and heterometallic compounds are synthetized with Ln:Ln' proportions of approximately 0,5:0,5, 0,25:0,75 and 0,75:0,25. All of them are luminescent under UV light: Tb is green, Eu red and Sm violet.

Due to the great properties of 2D materials, such as graphene, exfoliations of homometallic MOFs are carried out to achieve single-layer compounds dispersed in i-propanol.

Both for MOFs and for exfoliations, a luminescence study has been done to see where the electronic transitions responsible of their colour appear. Although f-f transitions are prohibited, due to the antenna effect of the ligand, the expected electronic transitions of Lanthanides can be observed in all compounds. Furthermore, Tb in heterometallic compounds acts as sensitizer, making the emission of the partner Ln' more intense.

After the confirmation of exfoliations luminescence, they are stamped. In a preliminary study, it is observed that through the fluorimeter the corresponding electronic transition appears, but it is not possible to see its luminescence at naked eye under UV light.

Keywords: MOFs, 2D Materials, Lanthanides, Antenna Effect, Sensitization, Exfoliations, Smart Inks.

2. RESUM

L'augment de falsificacions de documents o de monedes està esdevenint un problema per a la societat fent que s'hagi de plantejar una solució. Un possible mètode és el desenvolupament de tintes intel·ligents, que són luminescents sota determinades longituds d'ona.

Per a fer-ho, s'utilitzen MOFs de Lantànids amb estructura [$Ln(CH_3COO)(PhCOO)_2$] de Ln = Tb, Eu i Sm. Es sintetitzen compostos homometàl·lics i heterometàl·lics amb proporcions Ln:Ln' d'aproximadament 0,5:0,5, 0,25:0,75 i 0,75:0,25. Tots ells són luminescents sota la llum UV: el Tb verd, l'Eu vermell i el Sm violeta.

Degut a les grans propietats dels materials 2D, com el grafè, es duen a terme exfoliacions dels MOFs homometàl·lics per a aconseguir compostos d'una sola capa en dispersió amb i-propanol.

Tant per als MOFs com per a les exfoliacions es duu a terme un estudi de la luminescència per a veure on apareixen les transicions electròniques responsables de l'aparició de color. Tot i que les transicions f-f estan prohibides, degut a l'efecte antena del lligand, en tots els compostos es poden observar les transicions electròniques esperades dels Lantànids. També es pot observar que el Tb en els compostos heterometàl·lics actua de sensibilitzador fent l'emissió de la parella Ln' més intensa.

Un cop s'ha confirmat que les exfoliacions també presenten luminescència, es realitza la seva estampació, on en un estudi preliminar s'observa que a través del fluorímetre apareix la transició electrònica corresponent, però no és possible veure la seva luminescència a ull nuu sota la llum UV.

Paraules Clau: MOFs, Materials 2D, Lantànids, Luminescència, Efecte Antena, Sensibilització, Exfoliacions, Tintes intel·ligents.

3. INTRODUCTION

The metal-organic frameworks (MOFs) of Lanthanides are a good option for applications that need luminescent processes. These 2D MOFs can be exfoliated to use them in dispersion when the application requires it. Due to the increasing number of forgers, counterfeiting has become a big problem to be resolved. Inks made with lanthanides 2D MOFs could be a good option to avoid duplications of documents or currency due to they can be luminescent under specific light's wavelength making the documents or the currency most difficult to imitate.

3.1. LANTHANIDE CHEMISTRY

Lanthanides are the elements of the f-block, period 6 of the periodic table comprised between Lanthanum and Lutetium. They are the elements that have electrons in the electronic shell $4f^1$.

The electrons of 4f orbitals are not available to make a covalent bond since the atomic orbitals 4f are hidden or buried being only populated after filling the 5p and 6s shells following the Aufbau principle (Figure 1). Lanthanides are metals with no charge but they have a big tendency to react losing electrons with compounds that rapidly accept them. They react with acids and to form ions +3 and release hydrogen gas. With water they used to form oxides and hydroxides[2].

Lanthanides usually present an oxidation number +3, because the ionization beyond the ion M^{3+} is not possible. The sum of the first three ionization enthalpies is low so the elements are strongly electropositive. Exceptionally, cerium, praseodymium, and terbium can also present an oxidation number +4 and form +4 charged ions in chemical compounds that are strong oxidizers. Samarium, europium and ytterbium can lose 2 electrons to form +2 charged ions in compounds[1].

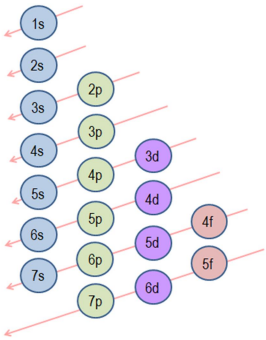

Figure 1. Aufbau principle showing how the shells are filled with electrons.

These elements also present the Lanthanide contraction that is the constant diminution of the radius along the series of elements as the atomic number is increased. This is due to the low shielding effect between electrons of the same electronic shield. In each increment of atomic number there is an increment of one electron in the 4f orbital shell[2]. The electron shielding is not very effective, even less than with the d electrons, for the orbital f shell. So there is an increment of effective nuclear charge for each electron added responsible of the reduction of the size[1].

The coordination numbers of these metals are high (>6) due to their big size. The different coordination numbers that they can have is determined principally by steric effects. The different coordination geometry for a specific coordination number is for the spatial requirements of the ligand. The atomic orbitals are buried and play a small role in the metal-ligand bond[2].

Lanthanides ions have special optical properties such sharp and stable emission peaks, long lifetime, intense luminescence and high colour purity so they are ideal luminescence emitters. For that reason, lanthanides ions are used for applications in labelling, light-emitting devices and fluorescence-tunable materials. The luminescent emissions of lanthanides ions are intensified using appropriate organic ligand molecules as light collectors. Eu^{3+} is one of the main ion used due to its strong red fluorescent emissions[3].

3.2. LUMINESCENCE

Some chemical species when irradiated with UV-visible light can populate an excited state that will relax emitting light. This phenomenon is called luminescence. The excitation to a luminescent excited state is depicted in a Jablonski diagram, as shown in Figure 2. To study the

luminescence of compounds, the sample is irradiated with a light that has a specific wavelength. The compound absorbs this light making a photon to excite from the ground state to an electronic state of higher energy, called excited state. Afterwards, this photon is relaxed to return to their ground state, emitting in the UV-visible wavelength[4].

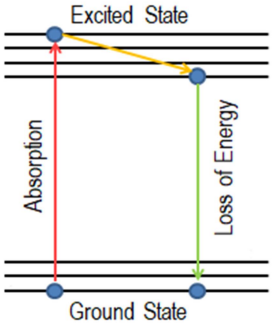

Figure 2. Jablonski diagram

Photons exhibit wave-particle duality, they have properties of both waves and particles. Considering photons as particles they act as electrons.

An electron is defined with four quantum numbers. The principal quantum number, n, which is related to the energy and to the average distance between the nucleus and the electron, measured in energy levels. The secondary quantum number, l, that determines the shape of the orbital. The magnetic quantum number, m, which describes the spatial orientation of the energy sublevel. Finally, the spin quantum number, s, which denotes the possible spins of the electron around its own axis. The spin and the motion of an electron can interact by spin-orbit coupling, in which case it is useful to couple its orbital (l) and spin (m) angular moments. This is due to the electron, in addition to orbiting around the nucleus, also rotates on itself.

The excitation to an excited state is very costly energetically for Lanthanides and usually direct excitation does not take place. A ligand, an organic group that absorbs UV-visible light, can be used to transfer the photon to the emitting excited state of the Lanthanide ion. The organic molecule that absorbs the incident light's energy is called chromophore or antenna[4].

The energy relaxation can occur by processes like phosphorescence and fluorescence, both comprised in photoluminescence. The main difference between them is that in fluorescence the energy of the incident light is absorbed emitting it immediately, while in phosphorescence there

is an energy storage allowing a slow emission during minutes or hours even if there is not incident excitation light.

Lanthanides present a very similar chemistry between them, as it was explained in a previous section, but each one has characteristic emissions. This is due to 5s and 5p orbitals are totally filled and present shielding. This shielding causes the energies of electronic states not to be dependent on their chemical environment. For this reason, the electronic transitions for Ln(III) always appear in the same energies regardless of the coordination compound, as shown in Figure 3[5,6].

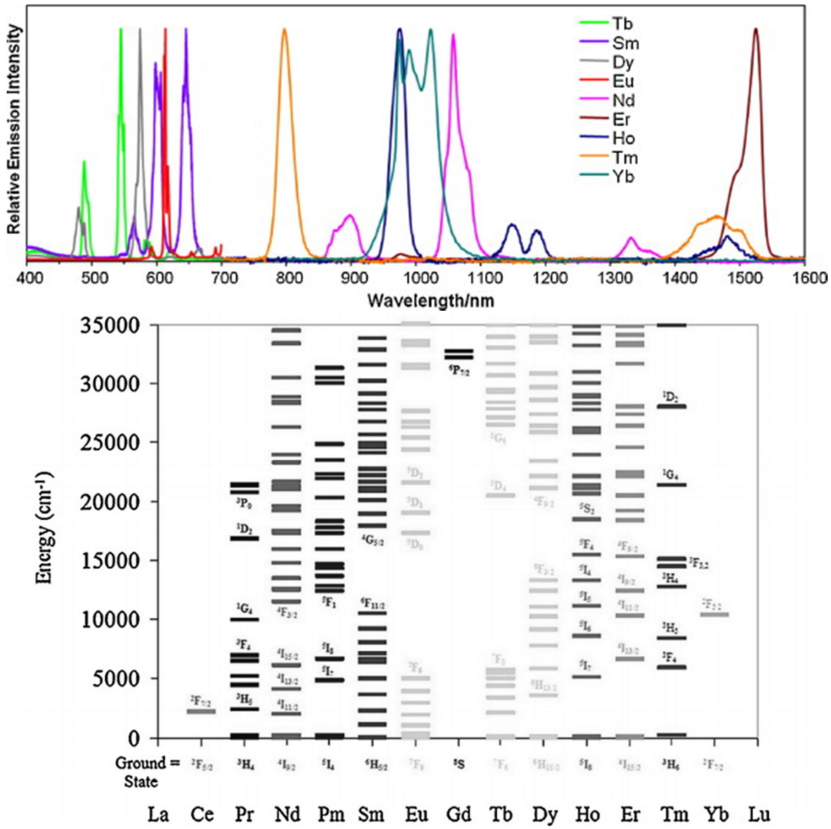

Figure 3. Electronic transitions of Lanthanides.
Images adapted from references:
Uh, H.; Petoud, S. Novel Antennae for the Sensitization of near Infrared Luminescent Lanthanide Cations. *Comptes Rendus Chim.* **2010**, *13* (6–7), 668–680.
D'Aléo, A.; Pointillart, F.; Ouahab, L.; Andraud, C.; Maury, O. Charge Transfer Excited States Sensitization of Lanthanide Emitting from the Visible to the Near-Infra-Red. *Coord. Chem. Rev.* **2012**, *256* (15–16), 1604–1620.

The intensity of the emission and absorption bands are conditioned by the selection rules that govern the system. The excited electron cannot change their spin during the transition. According to Laporte rule, transitions in the same subshell or orbitals of the same symmetry are not allowed, so f-f transitions are not permitted, thus the above mentioned Antenna effect is a key factor for Lanthanide emitting species and will be described in the next section.

Even so, selection rules are not always obeyed. In the case of Ln(III) , f-f transitions can make a change of the total spin of the molecule, except the transitions that take place in the IR. Even being prohibited by spin and by Laporte, the spherical symmetry of the ion is distorted when the metal is surrounded by the ligands and for this reason the symmetry of the states is modified.

3.2.1. Antenna effect

The f-f transitions are prohibited by Laporte, so the direct absorption of the light by the Ln(III) is not possible for symmetry reasons, and in many cases for changes of the total spin of the states as well. This results in low extinction coefficients $(\varepsilon\lambda)^4$.

The transitions of the studied MOF are due to Antenna effect. The organic chromophores of the ligands coordinated to the Ln(III) ions absorb light efficiently, they excite a photon and they transfer it to an excited state of the Ln(III). In the case of studied MOFs, phenyl from the benzoato ligands is the chromophore.

Generally, the transference occurs from the excited state of the ligand to the excited state of the metal. In ligands that have more than one chromophore, group interligand charge transfer processes (ILCT) can occur. In ligands that have two ligands with different chromophore groups in the same coordination complex charge transfer processes between ligands (LLCT) can occur[4].

Antenna effect only can occur if the excited state of the ligand have more energy than the excited state of the Ln(III) but those energies have to be close in energy as is shown in the Figure 4.

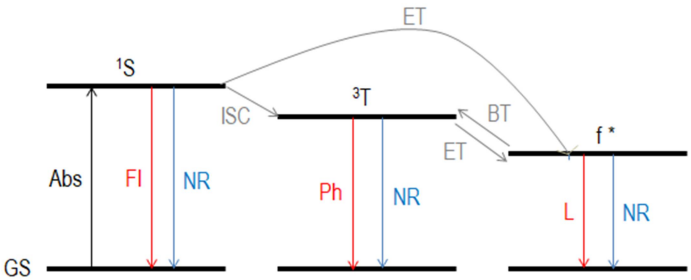

Figure 4. Modified Jablonski diagram that illustrates the antenna effect. Abs - absorption, Fl – fluorescence, L – luminescence, ISC- intersystem crossing, ET – energy transfer, BT – back energy transfer, NR – non-radiative deactivation, ^{1}S – first excited singlet State, ^{3}T – lowest excited triplet State, GS – ground State, f * - emissive f excited State.

To choose the ligand, the chromophore that the compound contains must be taken into account, since it must have a high extinction coefficient that ensures the absorption of light. The coordinating group that will allow its interaction with the ion Ln(III) must also be taken into account. The energetic transmission efficiency will be higher if the chromophore is part of the coordinating group, and therefore, it is directly connected with the Ln(III). In addition, complexes that have coordination numbers higher than eight have better energy transference efficiency due to possible coordination of deactivating solvent molecules are avoided[4].

If the compound has more than one chromophore group, it can present multiple antenna effects at different excitation wavelengths depending on the ligand, thus increasing the range of wavelengths of absorption.

3.3. 2D MATERIALS

The most important example of 2-Dimensional (2D) material is graphene. It is a single layer of graphite, the most common way of elemental carbon in elemental conditions[7].

Carbon can form different allotropes like graphite, diamond and amorphous carbon. Nowadays investigation is centred on fullerenes, carbon nanotubes and carbon nanofibers[8].

Graphene has extraordinary properties like electronic, mechanical, thermal, chemical, and optical characteristics that make it very interesting for new applications or to improve existing ones[8]. Until now, some areas of science are more developed like flexible electronics or conductive inks and other areas are in a conceptual stage like biomedicine or aerospatiale technologies[9].

Graphite has a planar layer structure. Their atoms are organized in honey comb lattices with a distance of 0,142nm between them. Three of the four electrons are involved into covalent bonds and the fourth one is free to move into the plane, making graphite electric conductor. Layers are connected between Van der Waals forces, thus allowing an easy separation between them. Their lattice system can be hexagonal (alpha) or rhombohedral (beta). One system can be transformed from one lattice system to the other one through mechanical or thermal treatment[9].

It can be considered an aromatic molecule, being part of the family of polycyclic aromatic hydrocarbons. It can be transformed into fullerene, rolled up in a nanotube or stacked into graphite[9].

There are two methods for synthetizing graphene: the bottom-up and the top-down shown in Figure 5[9]. The method bottom-up involve breaking stacked graphite layers to obtain single graphite layers. To do that it is necessary to break Van der Waals forces that keep the layers together. The keys of this method are to do an effective separation without damage individual layers, and to preserve the reagglomeration of the layers after the exfoliation[9]. This method is the followed in the study with Lanthanides 2D materials as the ones reported here

The other possible method for the synthesis of graphene is the bottom-up, which involves the synthesis from other sources containing carbon. This method needs high temperatures to promote high levels of graphitization. This type of approaches are more possible to present defects in graphene in comparison to top-down approaches, but their advantage is that is possible a direct growth in certain substrates suitable for applications. The best method depends on the final application that is given to the graphene[9].

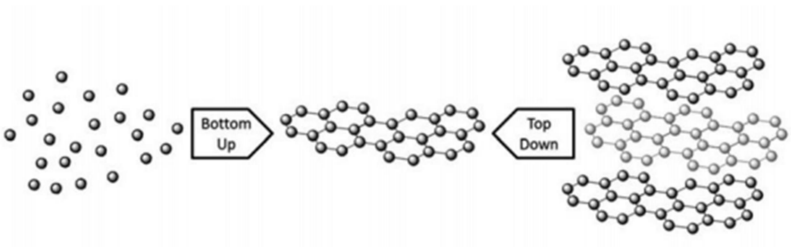

Figure 5. Both methods, top-down or bottom-up used to obtain 2D materials. Image adapted from reference Chaitoglou, S. Growth Study and Characterization of Single Layer Graphene Structures Deposited on Copper Substrate by Chemical Vapor Deposition.

The most important top-down approaches used to obtain graphene are micromechanical cleavage, exfoliation of graphite intercalation compounds (GICs), arc discharge, unzipping carbon nanotubes (CNTs), graphene oxide exfoliation, and solvent-base exfoliation[8].

Among the methods used for liquid-phase graphite exfoliation, the most popular is the ultrasound process (sonication) due to its low cost, versatility, scalability and the possibility to produce single layer, a few layer and multilayer graphene sheets The exfoliation using sonication is based on the mechanism when microbubbles are formed on the surface of graphite or close to it. These microbubbles results in secondary shock waves that hit the surface in fast and strong impact producing their sequential exfoliation[10].

After the discovery of amazing graphene properties, other 2D materials were investigated to improve the applications like 2D MOFs of Lanthanides. Compared to 3D bulk MOFs crystals, 2D have a larger surface area and more accessible active sites[11].

3.4. INKS

Documents or currency counterfeiting is a big problem to be resolved when that affects to the security or to the global economy. Due to exceptional optical properties of luminescent materials, they are promising materials in anticounterfeiting applications.

Counterfeiting is illegal and it is to make an imitation of something genuine with the intention of deceiving without permission from the owner. These illicit activities should be prevented improving the existing anticounterfeiting techniques and inventing new ones to avoid or difficult the duplication. For this reason, security printing is become important for reducing counterfeiting. New smart materials and advanced printing techniques are being developed to avoid forgers.

There are three anticounterfeiting techniques in security printing. The first one, through authenticating features recognizable by humans like watermarks, colour-shifting inks or visible security thread. The second technique is the choice of the substrate where to print. The third one, which is the reported here, is security ink. Most of these inks depend on UV radiation changing their colour at a specific wavelength or showing illumination. These inks are called smart inks[12].

Smart inks include the next features. Optical variable inks show diverse colour changing depending on the angle viewed. Holographic inks have an interference pattern on at least one

surface due to they contain regular shaped metal flakes. It can show coloured rainbow effect in the original exemplar, but if it is photocopied appears only black. Iridescent inks provide colour change with a flip-flop effect but do not have diffraction patterns. They are transparent when viewed at 90˚ but they have colour at 45˚[12].

Molecules used in formulation of printing inks are organic, inorganic and hybrid and they are easily synthesized from low-cost starting materials. For application as pigments in security printing lanthanide-doped molecules, conventional organic molecules, quantum dots and plasmonic nanomaterials are being explored.

The metal-organic frameworks (MOFs) exhibit high fluorescent efficiency for this reason is used in anticounterfeiting applications. MOFs are a class of inorganic-organic hybrid materials prepared from organic ligands and metal ions or metal clusters. These materials extend through repeating coordination compound entities in two or three dimensions and retain a small and uniform particle size.

Security inks consist of four components that are pigments, resins, solvents and additives. Pigments provide colour and are particles dispersed in the ink. The role of resins is to bind the ink together into a film and also bind it to the printed surface. Solvents are where the pigments are dispersed and aid in transport and drying of the ink[12]. A common solvent used in inks is the i-propanol, for this reason this is the solvent reported here.

3.5. PREVIOUS WORK AT GMMF ON 2D LANTHANIDE MOFS[13]

The microwave assisted synthesis of a bidimensional (2D) MOF of formula $[Dy(CH_3COO)(PhCOO)_2]_n$ was reported previously at this work by the group of magnetism and functional molecules (GMMF) of the University of Barcelona. This MOF was magnetically diluted analogue $[La_{0,9}Dy_{0,1}(CH_3COO)(PhCOO)_2]_n$. The magnetism and the luminescence of these MOFs were studied. Furthermore, both complexes were exfoliated into stable nanosheets by sonication.

The procedure to synthetize these MOFs is the following one. Hydrated $Dy(CH_3COO)_3$ and benzoic acid with a molar ratio of 1:2 is dissolved in MeCN/MeOH 1:1 mixture. The colourless solution is placed in the microwave reactor with 150W microwave pulse and at 125ºC. After cooling, the resulting white precipitate is separated and the colourless solution is placed for two to seven days at 40ºC in a furnace[13].

The crystal structure obtained consists of Van der Waals stacked nanosheets of a simple 2D MOF. As we can see in the Figure 6, Dy center has coordination number 8 and, according to shape, the coordination polyhedral is between a biaugmented trigonal prism and a distorted square antiprism. The binding mode of the acetate ligand is in a chelate, anti, anti-acetato, bridging three dysprosium ions. The bridging mode of benzoate ligands is in syn, syn-benzoato and bridge two dysprosium ions. Table 1 shows the crystallographic parameters for $[Dy(CH_3COO)(PhCOO)_2]$[14].

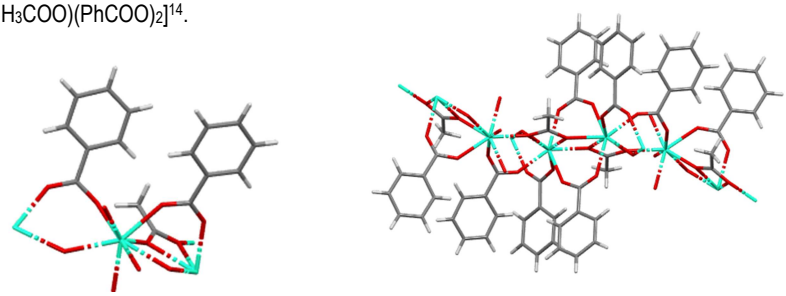

Figure 6. $[Dy(CH_3COO)(PhCOO)_2]$ and $[Dy(CH_3COO)(PhCOO)_2]_n$ structure.

PARAMETERS	$[Dy(CH_3COO)(PhCOO)_2]$
Distance Dy-O (Acetate) / Å	2,467
Distance Dy-O (Benzoate) / Å	2,303
Space group	P 2_1/c
a / Å	16,374
b / Å	12,597
c / Å	7,268
α / º	90
β / º	100,562
γ / º	90
V / Å^3	1473,72
R factor	4,68
Z	1
Crystal system	Monoclinic

Table 1[14]. $[Dy(CH_3COO)(PhCOO)_2]$ crystallographic parameters.

The luminescent study of Dysprosium shows that it is not luminescent. However, diluted species with Lanthanum present the emission transitions of Dy(III) when they are excited at 280nm, confirming the antenna effect from benzoate ligands. The absence of transitions in the complex of only Dysprosium is due to there is a quenching of luminescence between the Dy(III) centers[13].

This study also concludes that nanosheets of these MOFs can be obtained exfoliating them in isopropanol by sonication at 30ºC for 1 hour. Moreover, Tyndall effect can be observed in the suspension. The nanosheets are stable in suspension for at least two weeks[13].

4. OBJECTIVES

The main objective of this work is to synthetize the MOF $[Ln(CH_3COO)(PhCOO)_2]_n$ and heterometallic analogues using different lanthanides in order to study their luminescence and ultimately to use them as intelligent inks, which are luminescent at an specific wavelength and therefore difficult to imitate.

To achieve this goal, the following steps will be followed:

- The synthesis of homometallic and heterometallic MOFs.
- The exfoliation of the previous compounds.
- The characterization and the study of their luminescence.
- To stamp the exfoliated MOF in paper.

5. EXPERIMENTAL SECTION

All chemicals were obtained from commercial sources and used as received. Three types of synthesis have been done. Firstly, homometallic MOFs. After seeing that the compounds were the expected ones, the heterometallic ones had been done. Finally, the exfoliation of the homometallic MOFs with the aim to be stamped in a paper.

5.1. PREPARATION OF COMPOUNDS

The synthesis consists of the mixture of n moles of $Ln(CH_3COO)_3$ and 2n moles of PhCOOH, according to the following reaction. Quantities of each reagent are shown in Table 2.

$$Ln(CH_3COO)_3 + 2\ PhCOOH \rightarrow [Ln(CH_3COO)(PhCOO)_2] + 2\ CH_3COOH$$

The reaction is done with 2mL of CH_3OH and 2mL of CH_3CN as solvents in a microwave reactor tube. The mixture is put in the microwave with a pulse of 150W, a temperature of 125ºC and during 10 minutes. The microwave used is a *CEM Discover Microwave Reactor*. Then the reaction is cooled to room temperature and the precipitate obtained is decanted. The solution is left in the oven at 40ºC for several days and colourless crystals appear.

For heterometallic MOFs, the synthesis is the same as for homometallic compounds, but mixing two different $Ln(CH_3COO)_3$ while maintaining the proportions of n moles of $Ln(CH_3COO)_3$ for 2n moles of PhCOOH. The molar ratios used between Ln and Ln' were approximately of 0,25:0,75, 0,5:0,5 and 0,75:0,25. The exact ratio of Ln:Ln' present in the heterometallic compounds has been checked by elemental analyses and EDS analyses on the SEM microscope.

COMPOUND	$[Ln(CH_3COO)(PhCOO)_2]_n$	$Ln(CH_3COO)_3$ [mg]	$Ln'(CH_3COO)_3$ [mg]	PhCOOH [mg]	Yield [%]
1	Tb	88,1	-	64,0	29
2	Eu	172,3	-	127,4	83
3	Sm	85,0	-	63,40	70
4	$Sm_{0,5}Tb_{0,5}$	85,2	88,6	126,8	52
5	$Eu_{0,5}Tb_{0,5}$	85,30	88,30	127,5	30
6	$Eu_{0,5}Tb_{0,5}$	86,8	85,4	127,2	49
7	$Sm_{0,75}Tb_{0,25}$	127,5	45,2	126,3	69
8	$Sm_{0,25}Tb_{0,75}$	43,9	133,2	126,4	81
9	$Eu_{0,28}Tb_{0,72}$	44,0	115,9	115,9	28
10	$Eu_{0,75}Tb_{0,25}$	129,0	44,2	127,0	80

Table 2. Compounds prepared in this TFG, amounts of reagents and yields.

The prepared compounds have been characterized using the techniques listed in Table 3.

COMPOUND	$[Ln(CH_3COO)(PhCOO)_2]_n$	EA	PXRD	IR	Fluorescence
1	Tb			x	x
2	Eu	x	x	x	x
3	Sm	x	x	x	x
4	$Sm_{0,5}Tb_{0,5}$	x	x	x	x
5	$Eu_{0,5}Tb_{0,5}$	x	x	x	x
6	$Eu_{0,5}Tb_{0,5}$	x	x	x	x
7	$Sm_{0,75}Tb_{0,25}$	x	x	x	x
8	$Sm_{0,25}Tb_{0,75}$				x
9	$Eu_{0,28}Tb_{0,72}$				x
10	$Eu_{0,75}Tb_{0,25}$	x	x	x	x

Table 3. Characterization of the prepared compounds; EA: elemental analysis, PXRD: powder X-ray diffraction, IR: infrared spectroscopy.

5.2. PREPARATION OF EXFOLIATED 2D MOFS

The exfoliations are prepared from the previously synthetized homometallic compounds. The exfoliation consists of dispersing 1 mg of MOF in 10 mL of i-propanol. After that, two methods are followed. The first one sonicating the dispersion for 30 minutes at 30°C, and the second method sonicating for 60 minutes and at the same temperature. After the sonication, samples are centrifugated twice. Firstly, for one minute at 2000 rpm and decanted to eliminate big crystals, and finally centrifugated again for another minute at 6000 rpm and decanted to eliminate smaller microcrystals. The objective of the centrifugation is to obtain single layers of 2D MOF dispersed in i-propanol.

The sonicator used is an *Ultrasonic Cleaner VWR* and to centrifuge is used an *EBA 21 Hettich Zentrifugen*. Table 4 shows the centrifugation times applied to each compound.

Exfoliated sample	Solid used	Lanthanide	Time sonicating
11	1	Tb	30 minutes
12	1	Tb	60 minutes
13	2	Eu	30 minutes

14	2	Eu	60 minutes
15	3	Sm	30 minutes
16	3	Sm	60 minutes

Table 4. Exfoliated compounds and time of sonication for each one.

5.3. CHARACTERIZATION

The infrared spectroscopy has been done in the University of Barcelona at the department of Inorganic and Organic Chemistry using a *spectrophotometer FT-IR Nicolet iS5*. These technic is used to identify chemicals substances or functional groups.

The elemental analysis has been done in Scientific and Technological Centre of the University of Barcelona (CCiTUB). The analysis shows the percentage of carbon, hydrogen, nitrogen and sulphur respect to the total of the sample (Table 5).

COMPOUND	C [%] (exp.)	H [%] (exp)	N [%] (exp.)	C [%] (calc.)	H [%] (calc.)	N [%] (calc.)
1	-	-	-	41,74	2,85	0
2	41,87	2,86	0	41,88	2,97	0
3	41,54	2,78	0	41,56	3,05	0
4	41,78	2,87	0,69	41,60	3,08	0,45
5	41,02	2,83	0,71	41,31	3,12	0,41
6	41,89	2,86	0	41,68	3,02	0
7	41,27	3,01	0	41,45	3,05	0
8	-	-	-	41,98	2,86	0
9	-	-	-	42,00	2,87	0
10	41,20	2,97	0	41,50	3,01	0

Table 5. Elemental analysis for the prepared compounds (exp.: experimental results, calc.: calculated results).

COMPOUND	Ln/Ln'	FORMULA
1	-	$[Tb(CH_3COO)(PhCOO)_2]$

2	-	$[Eu(CH_3COO)(PhCOO)_2] \cdot (H_2O)_{0,25}$
3	-	$[Sm(CH_3COO)(PhCOO)_2] \cdot (H_2O)_{0,5}$
4	Sm/Tb=1,42	$[Sm_{0.58}Tb_{0.42}(CH_3COO)(PhCOO)_2] \cdot (CH_3CN)_{0,15}(H_2O)_{0,45}$
5	Eu/Tb=1,81	$[Eu_{0.64}Tb_{0.36}(CH_3COO)(PhCOO)_2] \cdot (CH_3CN)_{0,14}(H_2O)_{0,61}$
6	Eu/Sm=1,08	$[Eu_{0.5}Sm_{0.5}(CH_3COO)(PhCOO)_2] \cdot (H_2O)_{0,4}$
7	Sm/Tb=4,45	$[Sm_{0.82}Tb_{0.18}(CH_3COO)(PhCOO)_2] \cdot (H_2O)_{0,5}$
8	Sm/Tb=0,62	$[Sm_{0.38}Tb_{0.62}(CH_3COO)(PhCOO)_2]$
9	Eu/Tb=0,87	$[Eu_{0.47}Tb_{0.53}(CH_3COO)(PhCOO)_2]$
10	Eu/Tb=3,02	$[Eu_{0.75}Tb_{0.25}(CH_3COO)(PhCOO)_2] \cdot (H_2O)_{0,4}$

Table 6. Proportion of Ln/Ln' calculated with the EDS results and formulas concordant to the experimental results.

The SEM-EDS has done in the Scientific and Technological Centre of the University of Barcelona (CCiTUB). It provides high resolution images of the topography of the sample. It has an integrated detector that can identify quantitatively the weight percentage of each element of the sample. The EDS gives important information about de proportion of the metals in the heterometallic samples, shown in Table 6.

The Powder X-Ray Diffraction has been done in Scientific and Technological Centre of the University of Barcelona (CCiTUB). It can provide information on unit cell dimensions and is used for phase identification of a crystalline material. For the preparation of the sample, it was sandwiched between films of polyester of 3,6 microns of thickness. The instrument used is a *PANalytical X'Pert PRO MPD θ/θ* powder diffractometer of 240 millimetres of radius, in a configuration of convergent beam with a focalizing mirror and a transmission geometry with flat samples sandwiched between low absorbing films. The experiment conditions were: Cu Kα radiation (λ = 1,5418 Å), work power: 45 kV- 40mA, incident beam slits defining a beam height of 0,4 millimetres, incident and diffracted beam 0,02 radians *Soller* slits, *PIXcel* detector: active length=3,347º, 2θ/θ scans from 2 to 60 º2θ with a step size of 0,026 º2θ and a measuring time of 300 seconds per step.

The fluorescence study has been done using a *spectrofluorometer Nanolog™-Horiba Jobyn Yvon* in the University of Barcelona at the department of Inorganic and Organic Chemistry. It manifests the main electronic transitions responsible of the fluorescence of compounds.

The UV/Vis has performed in the University of Barcelona at the department of Inorganic and Organic Chemistry using an *UV-Visible Spectrophotometer Cary 100 Scan*. It provides information of the wavelength that is absorbed for the chromophore.

6. RESULTS AND DISCUSSION

6.1. SYNTHESIS

The synthesis of the MOF is an acid-base reaction between coordinated acetate ligands and benzoic acid. Benzoic acid is more acidic than acetic acid so the first one will lose the proton to form acetic acid in the products obtaining then the MOF expected.

The reaction is done in the microwave reactor. The microwave radiation is an electromagnetic radiation that is comprise between 10^8 and 10^{12} Hz.

The microwave radiations accelerate a lot of reactions, as they provide a specific environment with elevated temperatures and pressures. The microwave radiations interact with molecules' dipoles making them to align with the frequency of the applicated field. This field oscillates causing a constant disequilibrium of the molecules. The resistance of the molecules to the rotation dissipates in form of heat.

Another important advantage of this technique in front of conventional heating to make reactions is that the energy transfer to the reaction mixture is done through the involved species, making the heating homogeneous throughout the sample as it is shown in the Figure 7[15].

Moreover, the working temperatures are achieved in a few seconds in the microwave reactor, thus the power use is limited, reaction times are short and the reaction is done in one step limiting the amount of organic solvents used. Furthermore, no purification of the compound is required.

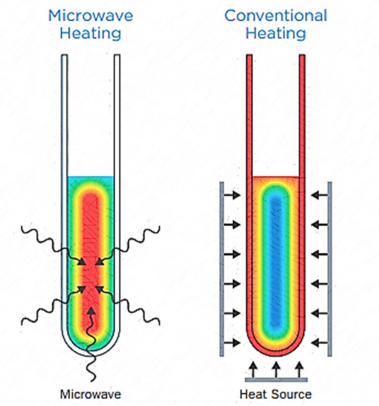

Figure 7. Homogeneous heating of microwave in front of conventional heating.
Image adapted from reference Synthesizer M. Microwave Synthesizer.

In heterometallic compounds, the metals can be distributed in different ways in the sample. As it was already explained, these MOFs can be exfoliated, obtaining an approximate shape of a honeycomb, placing a metal at each vertex. The most probable distribution of the two metals is randomly at the vertices. Another possible way is to distribute them by zones in the same 2D layer. The last option is placing one metal in each 2D layer. Figure 8 shows these three possible distributions.

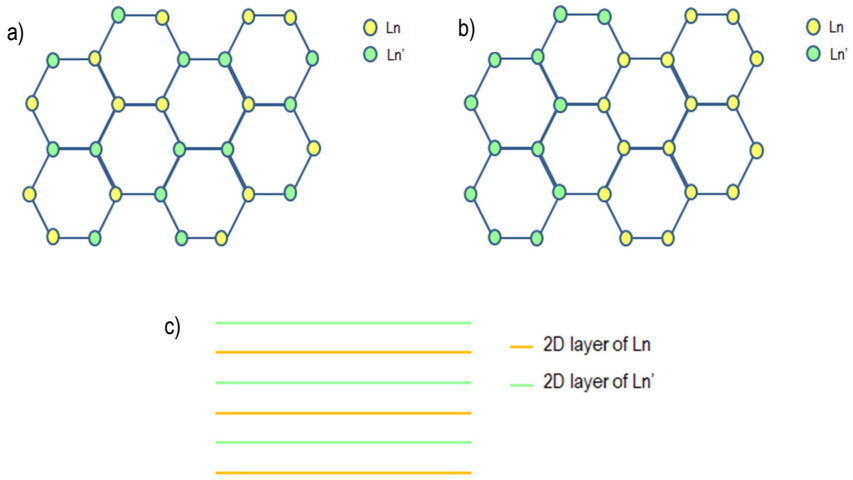

Figure 8. Distribution of metals in the sample. a) Random Distribution b) Distribution by zones
c) Layers Distribution

6.2. CHARACTERIZATION

The infrared spectrum gives important information about the complexation. The following figure shows the infrared spectra of the three homometallic compounds. There is not a peak in the 1600-1700cm^{-1} region where the free carboxylic acid C=O stretching appears. Instead, the two bands between 1350 and 1550cm^{-1} indicate the coordination of a carboxylate group to a metal, using both oxygen donors.

Furthermore, the three spectra of the homometallic complexes **1**(Tb), **2**(Eu), **3**(Sm) shown in Figure 9 are almost identical. The complex **1**(Tb) shows a residue of CH_3OH from incomplete drying of the solvent causing the appearance of a width peak at 3500cm^{-1}.

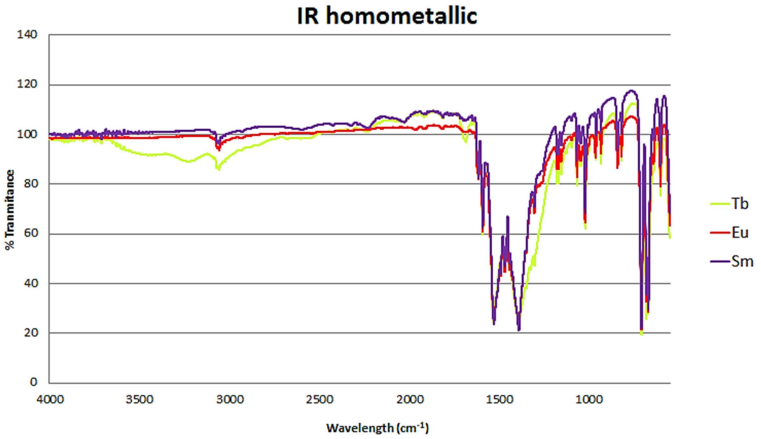

Figure 9. Infrared spectra of homometallic MOFs.

The elemental analysis of a sample can be done to obtain percentage of carbon, hydrogen and nitrogen. The analysis of sample 1 to 7 and 10 are within accepted error of the calculated values for the general formula [Ln(CH_3COO)($PhCOO)_2$], as shown in the Experimental Section Table 5. Thus, the nature of the prepared bulk materials 1 to 7 and 10 is confirmed by elemental analysis and IR. The small differences are mainly due to the fact that samples are wet. For the heterometallic cases, the relative amount of Lanthanides is slightly different to the expected one from the Ln:Ln' ratio use in the synthesis as shown in the Table 6 of the Experimental Section. The elemental analysis and EDS-SEM analyses have been used to ascertain the exact formula. Duplicates of the experiments should be done in order to confirm the exact formulae.

SEM images and EDS analysis on the SEM microscope were performed on all heterometallic samples 4 to 10. Figure 10 shows the SEM images of the solids 1-10 and Table 6 shows the EDS results. The SEM images show the formation of regular platelet crystals, of micrometer sizes, with the shortest dimension being extremely small, of the order of 0,5-2 micrometers. Compared to SEM image of Dy is possible to observe approximately the same shape of platelets. The images show both in the precipitates as well as the crystalline material obtained from the oven regular crystallite shapes, the precipitates show smaller platelets, while the crystalline material obtained after several days at 40ºC display larger platelets. This was previously observed by GMMF researcher's for the Dy 2D-MOF[13,14]. If a comparison of elemental analysis with EDS is done, it is possible to see that proportion of Lanthanides in the mixtures is not exactly the same that is expected from the reaction mixture in all compounds. This fact could be explained due to the distribution of Lanthanides in the structure or the relative solubilities of the two lanthanide ions used. Further studies should be done to ascertain whether the solid compositions are reproducible. The EDS is done at a very specific place of the sample, and both Lanthanides may not be distributed equally throughout the entire structure as it was explained in the Synthesis Section. Even so, it is possible to conclude that the variations are relatively small and that the MOFs obtained are the expected ones.

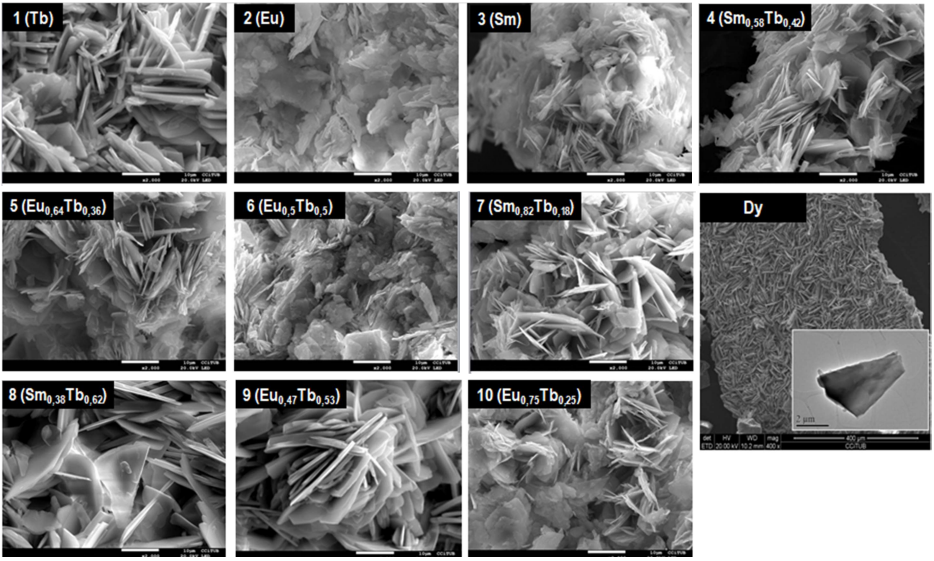

Figure 10. SEM images comparison of Dy complex in front of compounds 1 to 10. Dy[13] : SEM image obtained after 1 week at 40ºC, (inset) TEM image of a few monolayers exfoliated in i-PrOH. Complexes 1 to 10: SEM images obtained after a few days at 40ºC

Figure 11 shows the PXRD plots for complexes 2 to 7, 10 and Dysprosium complex, previously studied by GMMF researchers[13]. Through the results of PXRD a direct measurement of crystalline material is plotted, where X-Ray diffraction intensity is plotted against diffraction angular parameter (2θ). The spectra of all compounds have been compared with the calculated spectra of the crystalline structure of dysprosium MOF[14] done previously by other member of the group as it is explained at the previous work section. It is possible to see in the following representation that all spectra have the same shape. This is due all compound have the same structure, the only difference between them is the metal. In Appendix 1 are shown all PXRD spectra separated.

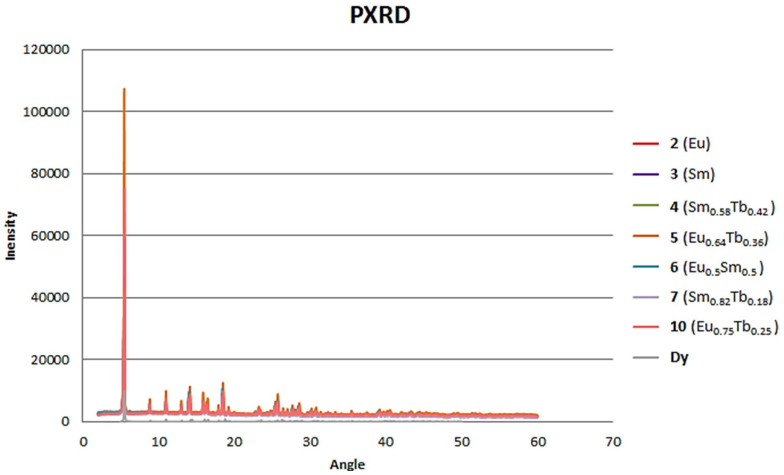

Figure 11. Diffraction pattern measured by PXRD

6.3. LUMINESCENCE

The compounds show different colours under ultraviolet light as it is possible to see in Figure 12. The compound **1**(Tb) is green, the compound **2**(Eu) is red and the compound **3**(Sm) is violet.

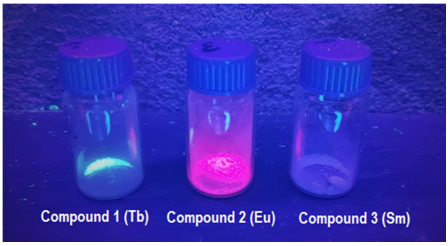

Figure 12. Colours of the compounds **1**(Tb), **2**(Eu) and **3**(Sm) under UV light.

The electronic transitions of complex **1**(Tb)[16] and complex **2**(Eu)[17] are the expected ones. Figure 13 shows that the intensity of the terbium transitions is higher than the europium transitions[18].

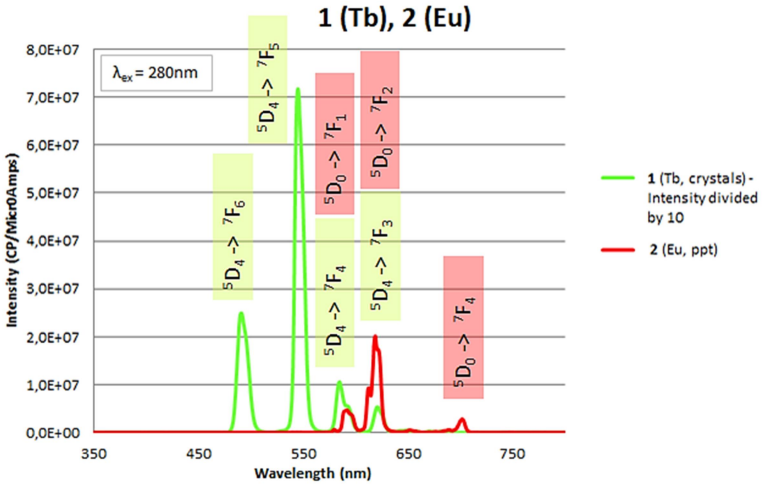

Figure 13. 1(Tb, green) and **2**(Eu, red) emission spectra.

The emission intensity of the compound **3**(Sm)[16] is lower compared with complexes **1**(Tb) and **2**(Eu). For this reason the peaks are not so well defined[18] as is showed in Figure14.

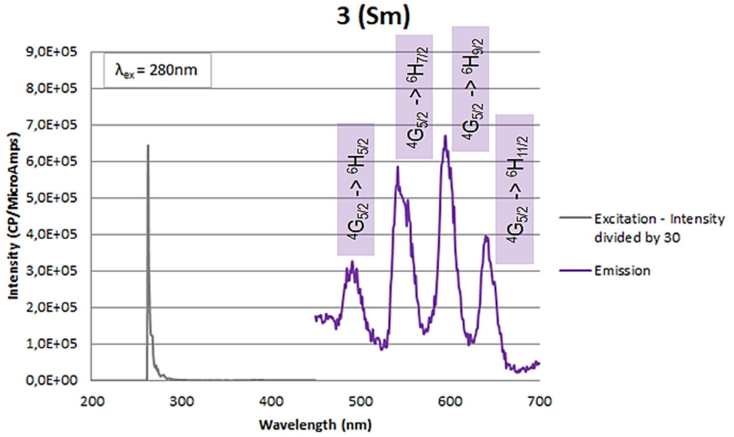

Figure 14. Excitation (grey) and emission (violet) spectra of compound **3**(Sm).

The absorption wavelength of the compound at 280 nm is due to the chromophore that absorbs the light is the benzoate and is the responsible of the antenna effect. To confirm that, an UV-Vis spectra is plotted in the Figure 15 comparing the signal of the sodium benzoate with the signal of one of the MOFs after exfoliation.

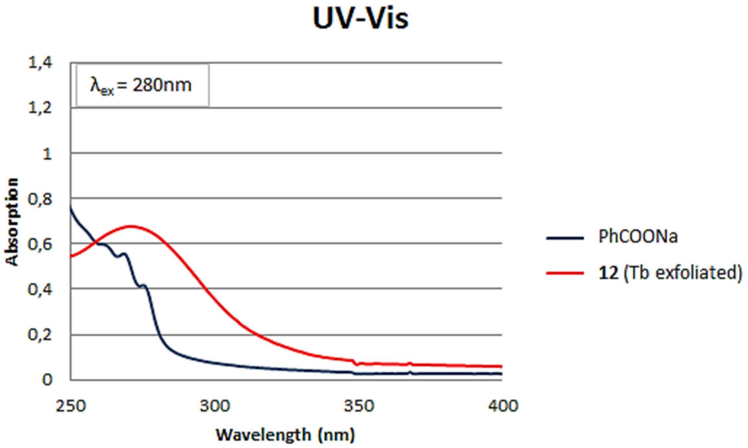

Figure 15. Spectra of UV-Visible for the complex **12**(Tb exfoliated) compared with spectra of PhCOONa.

For that reason, the maximum intensity of the peaks is reached with a radiation light of 280nm as is shown at the Figure 16 for **1**(Tb). When the excitation energy is shifted further away from this wavelength, the less intense are the emission peaks observed from the lanthanide ions.

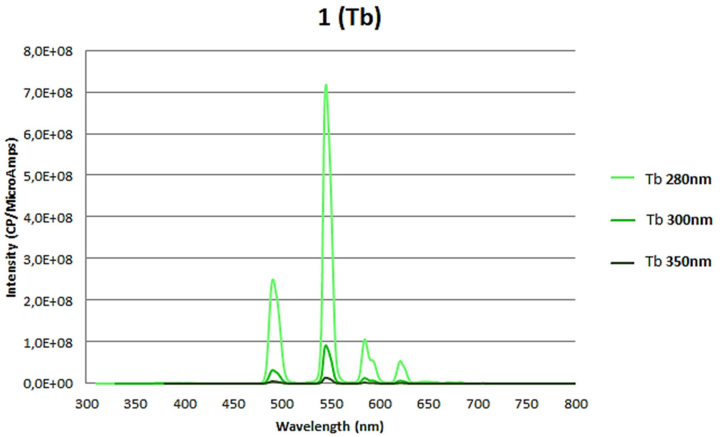

Figure 16. Electronic transitions for **1**(Tb) at different emission wavelengths.

The heterometallic compounds show different colours under ultraviolet light, shown in the Figure 17. The colour depends on the mixture of Lanthanides and on their ratio.

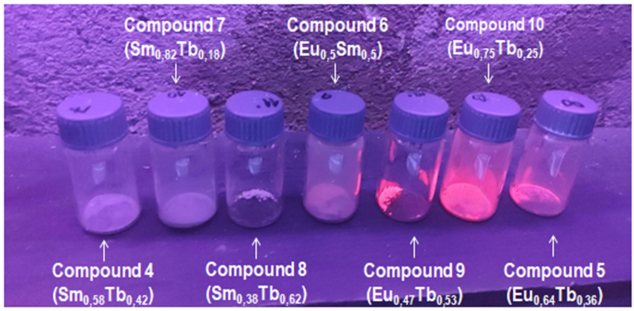

Figure 17. Colours of the heterometallic compounds under UV light.

Figure 18 shows the emission spectra of the complex **4**($Sm_{0,58}Tb_{0,42}$), **7**($Sm_{0,82}Tb_{0,18}$) and **8**($Sm_{0,38}Tb_{0,62}$), where represented showing only Samarium transitions. The peaks are not well defined due the low intensity that the transitions have. The emission of Samarium in the Sm/Tb heterometallic complexes is more intense than for the pure compound **3**(Sm). The higher Terbium content is reflected in more intense emission for Samarium due to the intermolecular energy transfer between Tb and Sm. This is a known effect called sensitization[19]. Figure 19 show the sensitization effect of Samarium by the presence of Terbium in the heterometallic complexes.

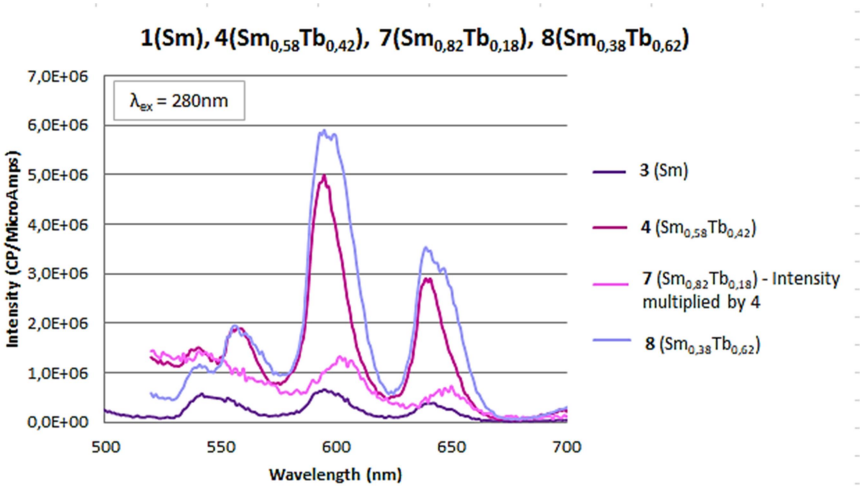

Figure 18. Emission spectra of **3**(Sm) and **4**($Sm_{0,58}Tb_{0,42}$), **7**($Sm_{0,82}Tb_{0,18}$), and **8**($Sm_{0,38}Tb_{0,62}$).

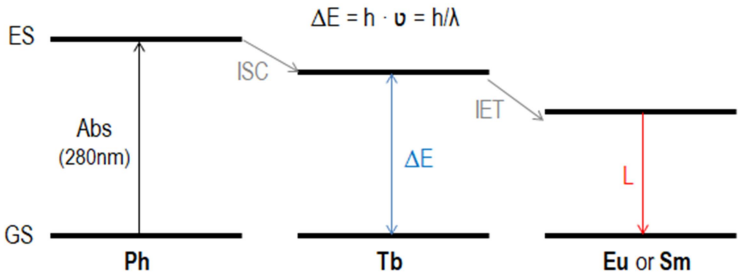

Figure 19. Modified Jablonski diagram that illustrates the sensitization effect. Abs - absorption, ISC – intersystem crossing, ΔE –energy difference between two energy levels, IET – intermolecular energy transfer, L – luminescence, GS – Ground State, ES - Excited State.

The spectra of the complex **5**($Eu_{0,64}Tb_{0,36}$), **9**($Eu_{0,47}Tb_{0,53}$) and **10**($Eu_{0,75}Tb_{0,25}$) presents only the europium transitions as it is represented in Figure 20. Again, sensitization of Eu emission by the presence of Tb is observed for the heterometallic complexes **5**($Eu_{0,64}Tb_{0,36}$), **9**($Eu_{0,47}Tb_{0,53}$) and **10**($Eu_{0,75}Tb_{0,25}$)[19]. However the maximum effect is achieved for the Eu:Tb 0,64:0,36 combination, compound **5**.

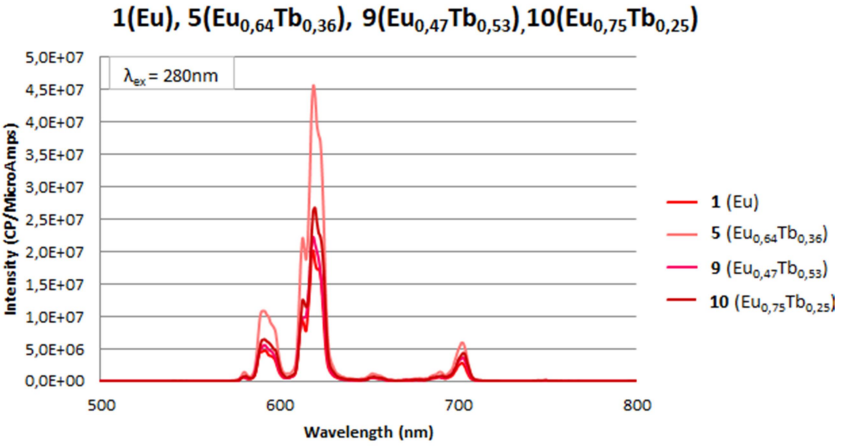

Figure 20. Emission spectra of **2**(Eu) and **5**($Eu_{0,64}Tb_{0,36}$), **9**($Sm_{0,47}Tb_{0,53}$), and **10**($Eu_{0,75}Tb_{0,25}$).

In the Figure 21 is plotted the luminescence spectra of the compound **6**($Eu_{0.5}Sm_{0.5}$) that shows only the transitions of the europium, due to the energy transfer from Sm to Eu[19].

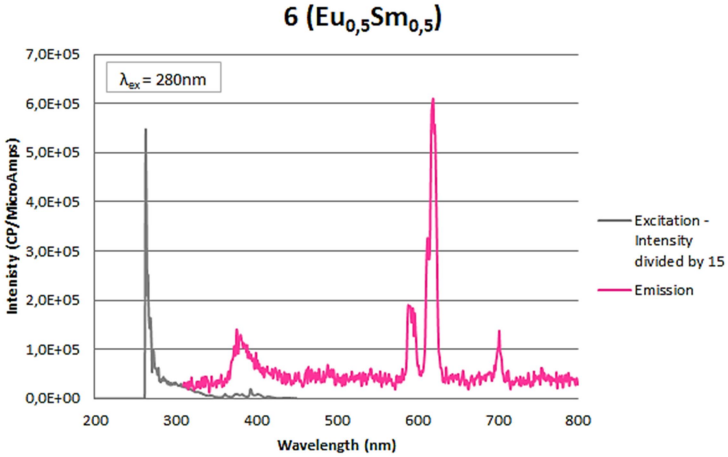

Figure 21. Emission spectra of compound **6**($Eu_{0,5}Sm_{0,5}$).

6.4. EXFOLIATIONS AND LUMINESCENCE OF NANOSHEETS

Exfoliation is achieved using the wet method of sonication. The sonication consists in applying to a liquid sample ultrasonic waves to shake the particles that are in it. It is possible to classify the acoustic waves depending on their vibration frequency (f): infrasounds (f<20Hz), audible sounds (20Hz<f<20kHz) and ultrasonic sounds (20kHz<f) that are out of the range that humans can hear and are the used ones in this technique[20].

The aim of sonicate the sample is to break Van der Waals bonds that are between crystal layers with the objective of getting monolayers. The sample is placed in a water bath where the waves are transferred by a series of compressions.

Waves' intensity is 3400 times higher in water than in air due the acoustic impedance, which is a measurement of how easy is for the wave to propagate through a particular medium[20].

After the sonication, the sample is centrifuged two times as it was explained in the experimental section in order to deposite the bigger crystals and to leave only the dispersed ones. The centrifuge uses the centripetal force to keep an object moving in a circular path in order to separate particles from solution. The components that have more density migrate away of centrifuge axis and the less dense components migrate towards the axis. The exfoliation process is exemplified in the cartoon of Figure 22.

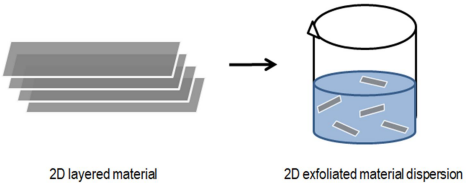

Figure 22. Wet exfoliation of a 2D MOF.

The 2D materials prepared here **1**(Tb), **2**(Eu) and **3**(Sm) can be exfolitated using this top-down method to obtain samples 11 to 16. All samples 11 to 16 show the Tyndall effect. The presence of nanoobjects in a solvent causes the light scattering that is an optical phenomenon that happens when bright light due to the presence of colloidal particles is forced to deviate from a straight trajectory by one or more paths. Tyndall effect takes place in a colloidal solution that contains particles of sizes smaller than the wavelength of visible light[21]. When the dispersion is irradiated with a red laser, the laser path can be observed on the transparent dispersion, as shown in Figure 23, this is called the Tyndall effect.

Figure 23. Tyndall effect.

For the exfoliations, two procedures were followed as it was explained at the experimental section. One sample was sonicated for 30 minutes (sample **11**(Tb30'), **13**(Eu30'), **15**(Sm30')) and other sample was sonicated for 60 minutes (sample **12**(Tb60'), **14**(Eu60'), **16**(Sm60')). The Figure 24 and Figure 25 show the intensity differences between the solid sample and between both exfoliations times for Tb and Eu 2D MOFs.

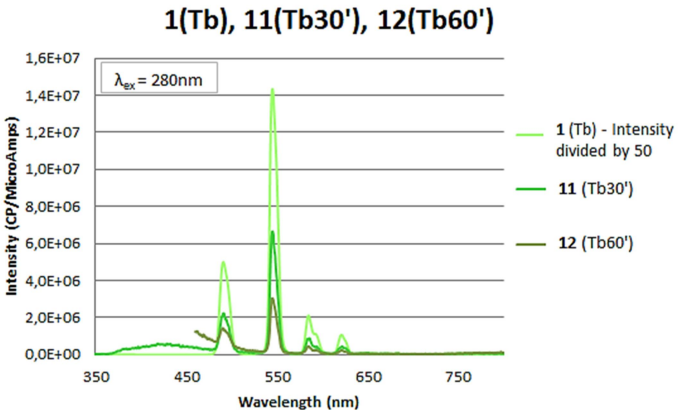

Figure 24. Electronic transitions for Terbium exfoliations.

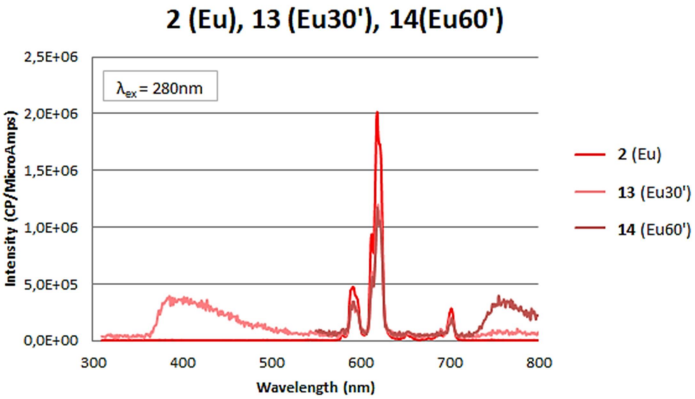

Figure 25. Electronic transitions for Europium exfoliations.

The emission of exfoliated **1**(Tb) show a clear dependence on the exfoliation time. Sample **11**(Tb30') exfoliated 30 minutes is more intense than sample **12**(Tb60') exfoliated 60 minutes. The emission of **2**(Eu) exfoliated for 30 and 60 minutes show nearly the same intensity. The reason for this observation is not clear and further experiments should be done in order to fully understand the exfoliation of the 2D MOFs prepared.

Samarium exfoliations do not present the expected Samarium transitions due they are less intense and the intensity in the exfoliated samples **15**(Sm30') and **16**(Sm60') is even lower. For this reason it is possible that the fluorometer is not able to detect them.

We attempted to stamp the compound **13**(Eu30') in a paper using a stamp. It was not possible to see any colour under the ultraviolet light as it was expected. After that, 10 drops were poured in to the paper one by one but no colour was seen under the ultraviolet light neither.

Both tests were characterized in the fluorometer but none of them have presented the expected transitions. We assume this is due to the low concentration of nanosheets in the dispersion. In order to try to fix this problem an attempt to prepare a more concentrated solution was undertaken. 5mg of **2**(Eu) were sonicated into 5mL of i-propanol, for 30 minutes and centrifuged following the above explained protocol. 10 drops of a 1mL micropipette were poured into a paper one by one. Although no colour was seen with the naked eye under ultraviolet light, it was possible to see the Europium transitions in the fluorometer, shown in the Figure 26.

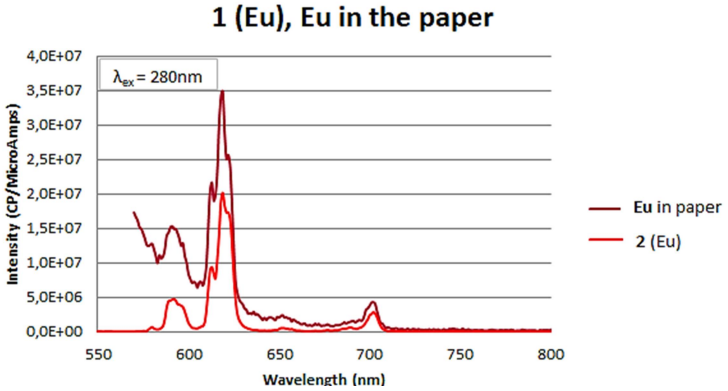

Figure 26. Comparison of compound **2**(Eu) transitions with the concentrated solution stamped to a paper.

7. CONCLUSIONS

The preparation of homometallic luminescent 2D-MOFs has been achieved. The prepared complexes **1**(Tb), **2**(Eu) and **3**(Sm) have been thoroughly characterized by IR, PXRD, EA, and luminescence studies.

The preparation of heterometallic luminescent Lanthanide based 2D-MOFs has been achieved for different ratios of Sm/Tb (compound **4**($Sm_{0,58}Tb_{0,42}$), **7**($Sm_{0,82}Tb_{0,18}$) and **8**($Sm_{0,38}Tb_{0,62}$)), Eu/Tb (compounds **5**($Eu_{0,64}Tb_{0,36}$), **9**($Eu_{0,47}Tb_{0,53}$) and **10**($Eu_{0,75}Tb_{0,25}$)), and Eu/Sm (compound **6**($Eu_{0,5}Sm_{0,5}$). The prepared complexes **1** to **10** have been thoroughly characterized by IR, PXRD, EA, SEM, EDS and luminescence.

The sensitization effect of Tb on Sm and Eu has been observed. This opens up further possibilities to exploit this effect in luminescent 2D materials,

Exfoliation of **1**(Tb), **2**(Eu) and **3**(Sm) has been successfully achieved. The dispersions of nanosheets show the Tyndall effect and the expected luminescence. Further experiments should be done to establish an exfoliation protocol that can ensure a large loading of nanosheets in the dispersion in order to achieve the use of these 2D materials in smart inks.

The presence of Europium in the paper after being stamped has been confirmed. The possibility of use these exfoliations for smart inks is still far. These results are the start for a deep investigation where a better characterization of the concentrated exfoliation should be done to ensure that in the solution there are only monolayers MOFs. Also a test of stamping with this solution using a stamp should be realized. Another possible test is to mix the exfoliated MOF with resins to bind them to the paper. Colorimetry studies should be done in order to ascertain the tuning of the observed colour for the heterometallic compounds.

8. REFERENCES AND NOTES

(1) Cotton, F. A.; Wilkinson, G. *Química Inorgánica Avanzada*, Limusa.; México, **1986**.

(2) G. Sharpe, A.; E. Housecroft, C. *Química Inorgánica*, 2nd ed.; Pearson, Ed.; Madrid, **2006**.

(3) Chen, B.; Xie, H.; Wang, S.; Guo, Z.; Hu, Y.; Xie, H. UV Light-Tunable Fluorescent Inks and Polymer Hydrogel Films Based on Carbon Nanodots and Lanthanide for Enhancing Anti-Counterfeiting. *Luminescence* **2019**, *34* (4), 437–443.

(4) Casanovas, B. Compostos de Coordinació Magnètics i/o Luminescents Derivats d'elements 3d o 4f: Cercant Sistemes Multipropietat (Doctoral Thesis). *Dr. Thesis* **2017**, 1–312.

(5) Uh, H.; Petoud, S. Novel Antennae for the Sensitization of near Infrared Luminescent Lanthanide Cations. *Comptes Rendus Chim.* **2010**, *13* (6–7), 668–680.

(6) D'Aléo, A.; Pointillart, F.; Ouahab, L.; Andraud, C.; Maury, O. Charge Transfer Excited States Sensitization of Lanthanide Emitting from the Visible to the Near-Infra-Red. *Coord. Chem. Rev.* **2012**, *256* (15–16), 1604–1620.

(7) I. Katsnelson, M.; Fasolino, A. Graphene: Basic Properties. In *2D Materials. Properties and Devices*; Cambridge University Press: California, University of Minnesota, 2017; pp 7–24.

(8) Lavin-Lopez, M. P.; Valverde, J. L.; Sanchez-Silva, L.; Romero, A. Solvent-Based Exfoliation via Sonication of Graphitic Materials for Graphene Manufacture. *Ind. Eng. Chem. Res.* **2016**, *55* (4), 845–855.

(9) Chaitoglou, S. Growth Study and Characterization of Single Layer Graphene Structures Deposited on Copper Substrate by Chemical Vapor Deposition.

(10) Alaferdov, A. V.; Savu, R.; Canesqui, M. A.; Kopelevich, Y. V.; da Silva, R. R.; Rozhkova, N. N.; Pavlov, D. A.; Usov, Y. V.; de Trindade, G. M.; Moshkalev, S. A. Ripplocation in Graphite Nanoplatelets during Sonication Assisted Liquid Phase Exfoliation. **2018**, 1–16.

(11) Jiang, Z. W.; Zou, Y. C.; Zhao, T. T.; Zhen, S. J.; Li, Y. F.; Huang, C. Z. Controllable Synthesis of Porphyrin-Based 2D Lanthanide Metal–Organic Frameworks with Thickness- and Metal-Node-Dependent Photocatalytic Performance. *Angew. Chemie - Int. Ed.* **2020**, *59* (8), 3300–3306.

(12) Muthamma, K.; Sunil, D.; Shetty, P. Luminophoric Organic Molecules for Anticounterfeit Printing Ink Applications: An up-to-Date Review. *Mater. Today Chem.* **2020**, *18*, 100361.

(13) González, J.; Sevilla, P.; Jover, J.; Echeverría, J.; Fuertes, S. A Multifunctional Dysprosium-Carboxylato 2D Metallorganic Framework. 1–5.

(14) González Sánchez, J. *Synthesis of Dy-Carboxylate 1-D and 2-D Complexes -TFG*; **2019**.

(15) Synthesizer, M. Microwave Synthesizer.

(16) Sun, X.; Huang, Z.; Guo, Y.; Zhou, S.; Liu, K. Tb3+ → Sm3+ Energy Transfer Induced Tunable Luminescence in Ba3MgSi2O8:Tb3+/Sm3+ Phosphors. *J. Lumin.* **2020**, *219* (November 2019), 116925.

(17) Jin, Y.; Wang, Y.; Wang, Y. Tuning Luminescence and Excellent Thermal Stability of Gd4.67Si3O13: Bi3+, Eu3+ with Energy Transfer from Bi3+ to Eu3+. *Ceram. Int.* **2020**, *46* (14), 22927–22933.

(18) Bettencourt-Dias, A. de. *Luminescence of Lanthanide Ions in Coordination Compounds and Nanomaterials*; Bettencourt-Dias, A. de, Ed.; John Wiley & Sons Inc.: United Kingdom, **2014**.

(19) Jiu, H.; Zhang, L.; Liu, G.; Fan, T. Fluorescence Enhancement of Samarium Complex Co-Doped

with Terbium Complex in a Poly(Methyl Methacrylate) Matrix. *J. Lumin.* **2009**, *129* (3), 317–319.
(20) Zhang, Y.; Abatzoglou, N. Review: Fundamentals, Applications and Potentials of Ultrasound-Assisted Drying. *Chem. Eng. Res. Des.* **2020**, *154*, 21–46.
(21) Xiao, W.; Deng, Z.; Huang, J.; Huang, Z.; Zhuang, M.; Yuan, Y.; Nie, J.; Zhang, Y. Highly Sensitive Colorimetric Detection of a Variety of Analytes via the Tyndall Effect. *Anal. Chem.* **2019**, *91* (23), 15114–15122.

9. ACRONYMS

MATERIALS

MOFs	Metal-Organic Frameworks
2D	Two-Dimensional
3D	Three-Dimensional

LUMINESCENCE

Abs	Absorption
FI	Fluorescence
L	Luminescence
ISC	Intersystem Crossing
ET	Energy Transfer
IET	Intermolecular Energy Transfer
BT	Back Energy Transfer
NR	Non-Radiative Deactivation
GS	Ground State

CARBON RELATED

GICs	Graphite Intercalation Compounds
CNTs	Carbon Nanotubes

TECHNIQUES

EA	Elemental Analysis

PXRD	Powder X-Ray Diffraction
IR	Infrared Spectroscopy
SEM-EDS	Scanning Electron Microscopy – Energy Dispersive X-Ray Spectroscopy
UV-Vis	Ultraviolet-Visible Spectroscopy

ORGANIZATIONS

GMMF	Group of Magnetism and Functional Molecules
CCiTUB	Centre Científic i Tecnològic de la UB

APPENDICES

APPENDIX: ALL PXRD SPECTRA

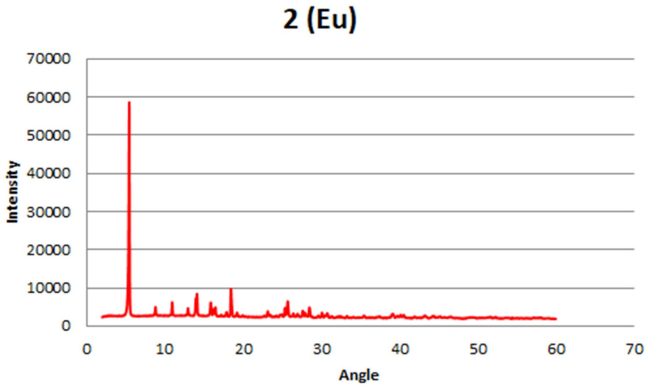

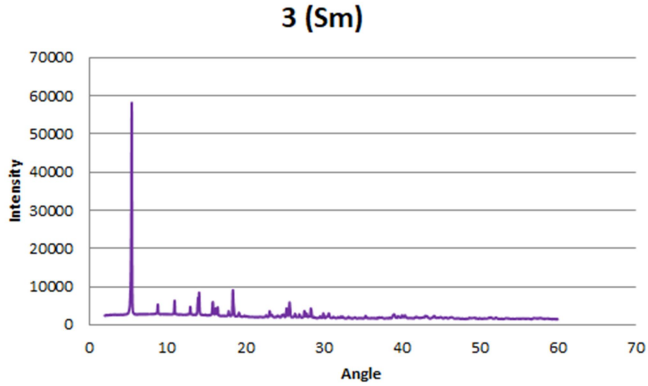

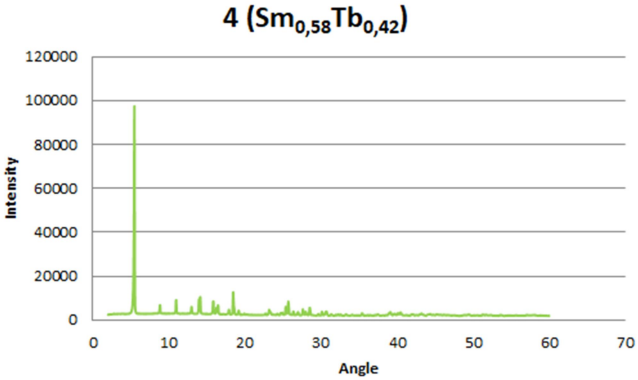
4 (Sm0,58Tb0,42)
120000
100000
80000
60000
40000
20000
0
Intensity
0
10
20
30
40
50
60
70
Angle

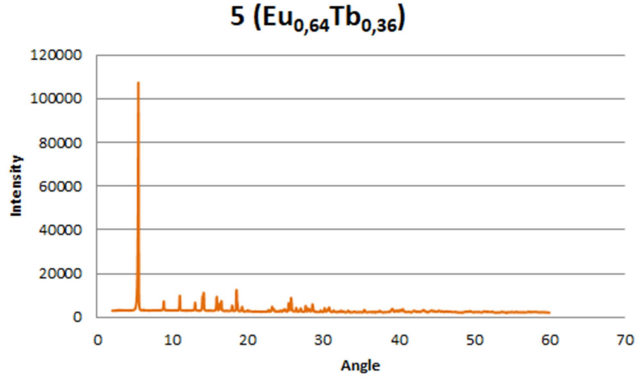
5 (Eu0,64Tb0,36)
120000
100000
80000
60000
40000
20000
0
Intensity
0
10
20
30
40
50
60
70
Angle

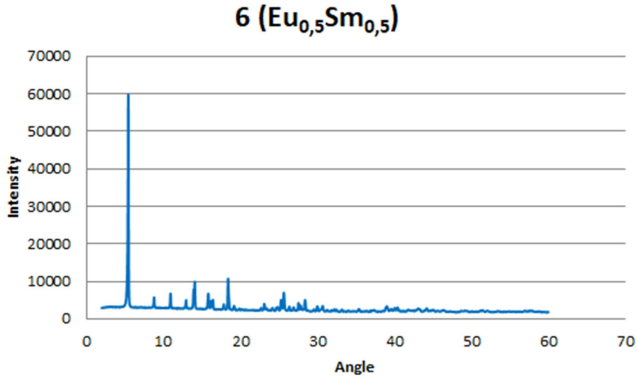
6 (Eu0,5Sm0,5)
70000
60000
50000
40000
30000
20000
10000
0
Intensity
0
10
20
30
40
50
60
70
Angle

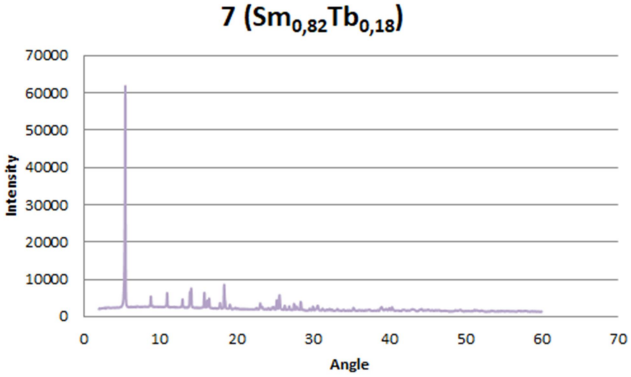
7 ($Sm_{0,82}Tb_{0,18}$)
Intensity
70000
60000
50000
40000
30000
20000
10000
0
0
10
20
30
40
50
60
70
Angle

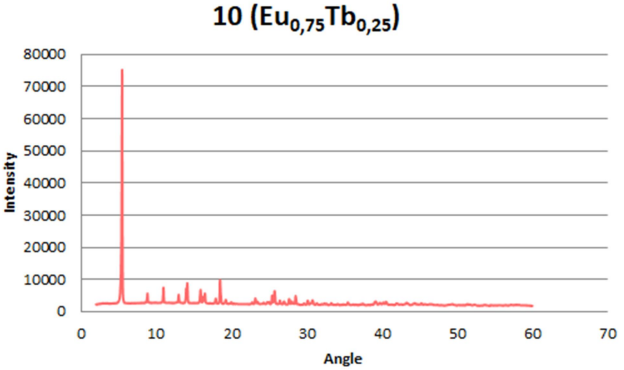
10 ($Eu_{0,75}Tb_{0,25}$)
Intensity
80000
70000
60000
50000
40000
30000
20000
10000
0
0
10
20
30
40
50
60
70
Angle

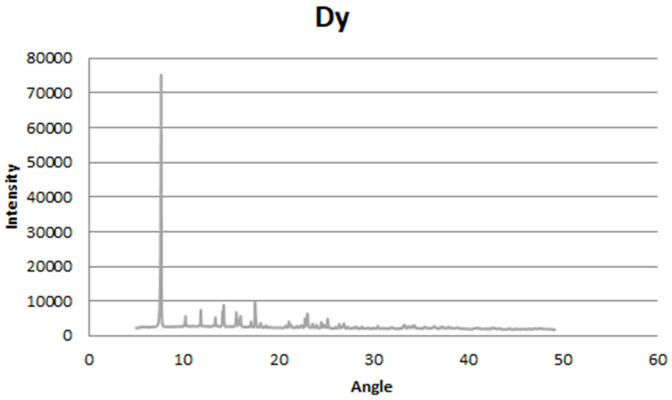
Dy
Intensity
80000
70000
60000
50000
40000
30000
20000
10000
0
0
10
20
30
40
50
60
Angle